Université Libre de Bruxelles

Institut de Recherches Interdisciplinaires et de Développements en Intelligence Artificielle

Advanced Calibration of Omni-directional Cameras Based on Supervised Machine Learning

T. Soleymani, V. Trianni, and M. Dorigo

IRIDIA – Technical Report Series

Technical Report No.
TR/IRIDIA/2013-012

October 2013

IRIDIA – Technical Report Series
ISSN 1781-3794

Published by:
IRIDIA, *Institut de Recherches Interdisciplinaires et de Développements en Intelligence Artificielle*
Université Libre de Bruxelles
Av F. D. Roosevelt 50, CP 194/6
1050 Bruxelles, Belgium

Technical report number TR/IRIDIA/2013-012

Advanced Calibration of Omni-directional Cameras Based on Supervised Machine Learning

T. Soleymani, V. Trianni, and M. Dorigo

IRIDIA

October 2013

Introduction

This report explains our approach for calibrating the omni-directional cameras. The omni-directional cameras are normally subject to error such as mirror deflection and image distortion. Therefore, mapping the acquired image coordinates of the objects to the real-world coordinates is not straightforward. In this approach, we employ a machine learning algorithm [1] to obtain two hypotheses that map with high accuracy the image coordinates to the real-world coordinates. We specifically implemented our algorithm for the Marxbots. More information about this robot is available in [2].

Preliminaries

We need first to acquire a set of training data. To this end, we use multiple colorful marks which are in two colors. We arrange them on the floor in a special grid pattern as shown in the Fig. 1.

Then, we use the image processing algorithm (already developed at IRIDIA) to detect the marks in different color channels, which here are red and green. The binary image of the marks detected by the omni-directional camera is illustrated in Fig. 2. We obtain the coordinates of 128 marks in the image that by are by default available in the polar coordinate system. The data of each mark corresponds to one observation.

The set of training data is defined as

$$S = \left\{ (r_m^{(i)}, \theta_m^{(i)}, r_r^{(i)}, \theta_r^{(i)}); \quad i \in \{1, \ldots, M\} \right\} \tag{1}$$

where M is the number of observations, $r_m^{(i)}$ and $\theta_m^{(i)}$ are the input values (i.e., polar components in the image coordinate system), and $r_r^{(i)}$ and $\theta_r^{(i)}$ are the target values (i.e., polar components in the real-world coordinate system), all for the ith observation.

Association

In this section, we associate each mark in the image to the corresponding one in the real-world. In general, we need to define an appropriate index function, and then by employing an optimization algorithm associate M points in the image space to the M points in the real-world space. This index function must be defined in a way that its global minimum corresponds to the correct association. Defining such a function for the unidentified marks are difficult. Fortunately, for the chosen resolution and configuration (in two different channels), we can exploit the continuity of two spaces and apply a geometric association. We first cluster the marks into 13 groups based on the value of their x-coordinates and their color. These groups are

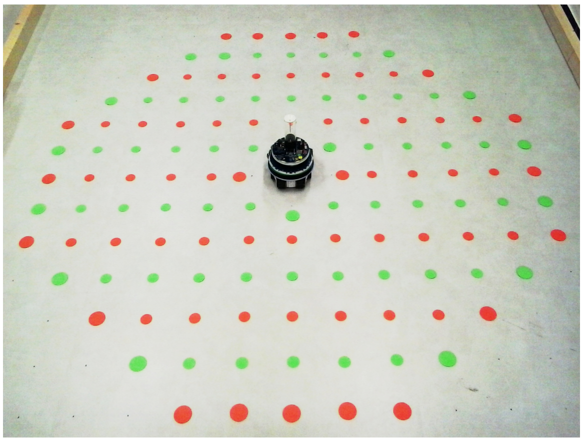

Figure 1: Configuration of 128 marks around a Marxbot.

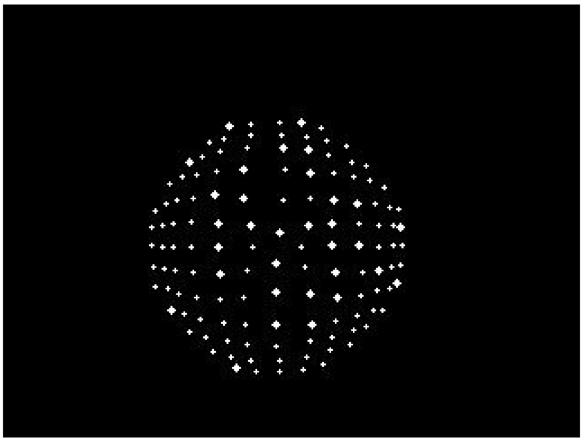

Figure 2: Output of image processing detected by omni-directional camera in a binary image.

distinguishable in the real-world and image as members of each group posses x-coordinates in a fixed interval and have similar colors. Note that these groups have different sizes.

Then, we associate each member in the each group to the corresponding one in the real-world based on their y-coordinates by moving from one direction. The center of mass of marks in the two channels and the association are depicted in the Fig. 3 and Fig. 4 respectively.

Deriving the hypotheses

In this section, we use a supervised machine learning algorithm to obtain the calibration hypotheses. The hypotheses are functions $h_1 : X \to Y_1$ and

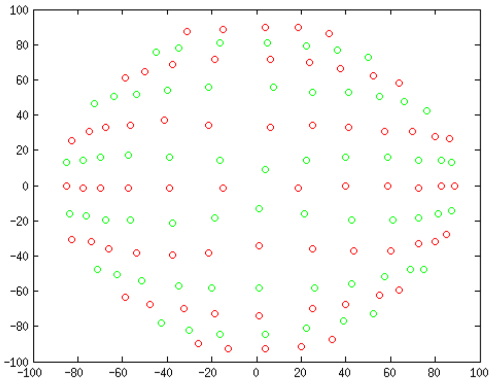

Figure 3: Center of masses of the marks in 2 channels.

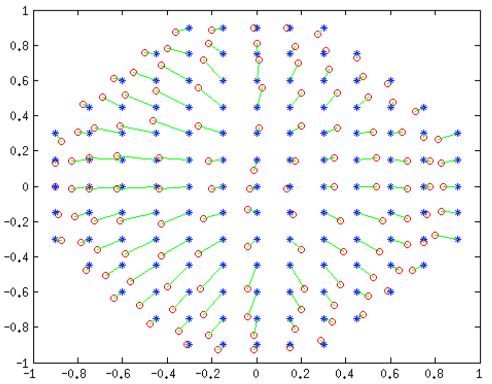

Figure 4: Association of marks in the image to the corresponding one in the real-world (here shown by overlapping them).

$h_2 : X \rightarrow Y_2$ where X is the input space, and Y_1 and Y_2 are the target spaces.

The domain of theses hypotheses is image coordinates, and their range is real-world coordinates. The desired coordinate system for our application is Cartesian, and the polar coordinate system that our observations are expressed in it is not appropriate because it causes a discontinuity in the hypotheses at $\pm\pi$.

We express the training data in the Cartesian coordinate system (these coordinates are also used for the association as mentioned earlier)

$$\begin{aligned} x_m^{(i)} &= r_m^{(i)} cos(\theta_m^{(i)}), \\ y_m^{(i)} &= r_m^{(i)} sin(\theta_m^{(i)}), \\ x_r^{(i)} &= r_r^{(i)} cos(\theta_r^{(i)}), \\ y_r^{(i)} &= r_r^{(i)} sin(\theta_r^{(i)}) \end{aligned} \tag{2}$$

where $i \in \{1, \dots, M\}$. Thus, the new set of training data is written as

$$S' = \left\{ (x_m^{(i)}, y_m^{(i)}, x_r^{(i)}, y_r^{(i)}); \quad i \in \{1, \dots, M\} \right\} \tag{3}$$

Let us define eight features as the following

$$\begin{aligned} &x_1 = x_m, \quad x_2 = x_m^2, \quad x_3 = x_m^3, \quad x_4 = x_m^4, \\ &x_5 = y_m, \quad x_6 = y_m^2, \quad x_7 = y_m^3, \quad x_8 = y_m^4, \\ &x_9 = x_m y_m, \quad x_{10} = x_m^2 y_m, \quad x_{11} = x_m y_m^2 \end{aligned} \tag{4}$$

where x_m and y_m are x- and y-coordinates in the image.

The target variables are the real-world coordinates

$$y_1 = x_r, \quad y_2 = y_r \tag{5}$$

where x_r and y_r are x- and y-coordinates in the real-world.

We assume that the maps are polynomial functions of degree four. Therefore, we can write the hypotheses as

$$\begin{aligned} h_1 = {} & \theta_{1,0} + \theta_{1,1}x_1 + \theta_{1,2}x_2 + \theta_{1,3}x_3 + \theta_{1,4}x_4 + \theta_{1,5}x_5 + \theta_{1,6}x_6 \\ & + \theta_{1,7}x_7 + \theta_{1,8}x_8 + \theta_{1,9}x_9 + \theta_{1,10}x_{10} + \theta_{1,11}x_11 + \theta_{1,12}x_{12} \end{aligned} \tag{6}$$

$$\begin{aligned} h_2 = {} & \theta_{2,0} + \theta_{2,1}x_1 + \theta_{2,2}x_2 + \theta_{2,3}x_3 + \theta_{2,4}x_4 + \theta_{2,5}x_5 + \theta_{2,6}x_6 \\ & + \theta_{2,7}x_7 + \theta_{2,8}x_8 + \theta_{2,9}x_9 + \theta_{2,10}x_{10} + \theta_{2,11}x_11 + \theta_{2,12}x_{12} \end{aligned} \tag{7}$$

where $\theta_{1,i}$ and $\theta_{2,i}$, $i \in \{0, \dots, 10\}$ are the unknown parameters.

Let us define two index functions as the following

$$J_1 = \frac{1}{2m} \sum_{i=1}^{M} (h_1^{(i)} - y_1^{(i)})^2 \tag{8}$$

$$J_2 = \frac{1}{2m} \sum_{i=1}^{M} (h_2^{(i)} - y_2^{(i)})^2 \tag{9}$$

where $h_1^{(i)}$ and $h_2^{(i)}$ are the hypotheses calculated for the ith observation. Our goal is to obtain the optimal gains which minimize the index functions respectively, that is Θ_1 and Θ_2.

$$\begin{aligned} \Theta_1 &= [\theta_{1,0}\ \theta_{1,1}\ \theta_{1,2}\ \theta_{1,3}\ \theta_{1,4}\ \theta_{1,5}\ \theta_{1,6}\ \theta_{1,7}\ \theta_{1,8}\ \theta_{1,9}\ \theta_{1,10}\ \theta_{1,11}\ \theta_{1,12}] \\ \Theta_2 &= [\theta_{2,0}\ \theta_{2,1}\ \theta_{2,2}\ \theta_{2,3}\ \theta_{2,4}\ \theta_{2,5}\ \theta_{2,6}\ \theta_{2,7}\ \theta_{2,8}\ \theta_{2,9}\ \theta_{2,10}\ \theta_{2,11}\ \theta_{2,12}] \end{aligned} \tag{10}$$

In order to obtain the optimal gains, we need to solve the following equations iteratively and simultaneously for all observations

$$\text{repeat until convergence} \quad \{ \\ \theta_{1,j} := \theta_{1,j} - \alpha \frac{\partial}{\partial \theta_{1,j}} J_1 \\ \} \tag{11}$$

$$\text{repeat until convergence} \quad \{ \\ \theta_{2,j} := \theta_{2,j} - \alpha \frac{\partial}{\partial \theta_{2,j}} J_2 \\ \} \tag{12}$$

where α is the learning coefficient.

Evaluation

In this section, we implement the algorithm, and obtain the optimal gains of the hypotheses. We evaluated the equations 11 and 12 for a set of observations acquired by a Marxbot. The index functions as the functions of the iterations are illustrated in the Fig. 5 and Fig. 6. As it is seen, these functions converge to minimal values after some iterations. These minimums correspond to the optimal gains.

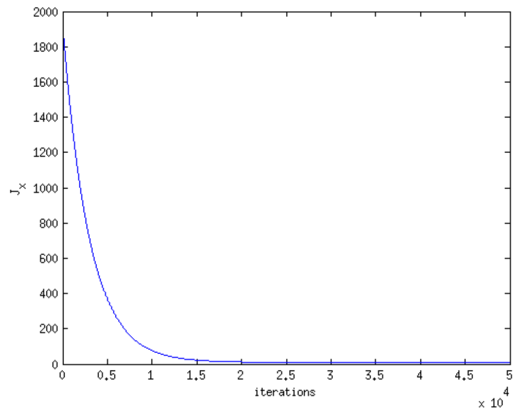

Figure 5: Index function J_1 versus iterations.

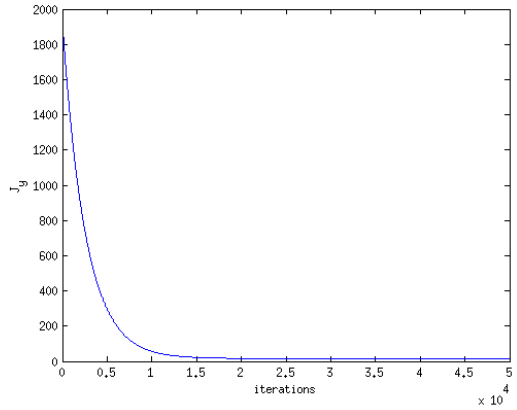

Figure 6: Index function J_2 versus iterations.

The optimal gains associated to our observations are

$$\Theta_1 = [0.0139,\ 1.0940,\ 0.03977,\ 0.3657,\ 0.0011,\ 0.0008,\ -0.0141,\ 0.0008,\ -0.00655,\ 0.0061,\ 0.00248,\ 0.1339]$$

$$\Theta_2 = [0.0120,\ -0.0128,\ -0.0049,\ -0.0021,\ -0.0010,\ 1.0923,\ -0.0025,\ 0.3664,\ -0.0060,\ 0.0200,\ 0.1307,\ -0.0008] \tag{13}$$

Now, we evaluate the predictions of the hypotheses for a new value as an input. The location of the mark, as shown in the Fig. 7, is

$$\begin{aligned} x_r &= 42.50 \text{ cm} \\ y_r &= 36.00 \text{ cm} \end{aligned} \tag{14}$$

The predictions of the hypotheses are

$$\begin{aligned} h_1 &= 46.06 \text{ cm} \\ h_2 &= 38.83 \text{ cm} \end{aligned} \tag{15}$$

We refer to e_1 and e_2 as the errors of the first and second hypotheses, and define them as

$$\begin{aligned} e_1 &= \frac{x_r - h_1}{x_r} \times 100 = 8.38\% \\ e_2 &= \frac{y_r - h_2}{y_r} \times 100 = 7.76\% \end{aligned} \tag{16}$$

We can also express the location of test mark in the polar coordinate system

$$\begin{aligned} r_r &= 55.70 \text{ cm} \\ \theta_r &= 40.27 \text{ deg} \end{aligned} \tag{17}$$

The predictions in the polar coordinate system are

$$\begin{aligned} h_r &= 60.24 \text{ cm} \\ h_\theta &= 40.13 \text{ deg} \end{aligned} \tag{18}$$

Finally, the errors in the polar coordinate system are

$$\begin{aligned} e_r &= \frac{r_r - h_1'}{r_r} \times 100 = 8.16\% \\ e_\theta &= \frac{\theta_r - h_2'}{\theta_r} \times 100 = 0.34\% \end{aligned} \tag{19}$$

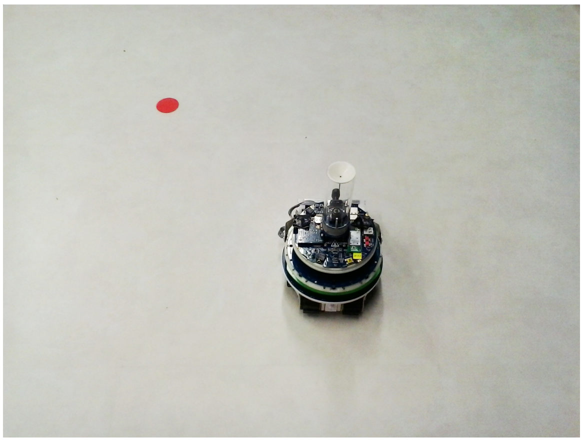

Figure 7: Test mark.

These estimates are satisfactory for our applications. However, one can get better result by introducing more marks in the sample set while using the same approach.

Bibliography

[1] M. Christopher, Pattern Recognition and Machine Learning, Springer, 2006

[2] Bonani, M. and Longchamp, V. and Magnenat, S. and Retornaz, P. and Burnier, D. and Roulet, G. and Vaussard, F. and Bleuler, H. and Mondada, F., *"The marXbot, a miniature mobile robot opening new perspectives for the collective-robotic research"*, Intelligent Robots and Systems (IROS), 2010 IEEE/RSJ International Conference on, 2010, p4187-4193.